Rotational and Translational Motion of Benzene in ZIF-8 Studied by 2 H NMR: Estimation of Microscopic Self-Diffusivity and Its Comparison with Macroscopic Measurements

ARTICLE *in* THE JOURNAL OF PHYSICAL CHEMISTRY C · MAY 2014

Impact Factor: 4.77 · DOI: 10.1021/jp5026834

5 AUTHORS, INCLUDING:

Daniil Kolokolov
Boreskov Institute of Catalysis
28 PUBLICATIONS **305** CITATIONS
SEE PROFILE

Lisa Diestel
Helmholtz-Zentrum Berlin
9 PUBLICATIONS **71** CITATIONS
SEE PROFILE

Dieter Freude
University of Leipzig
184 PUBLICATIONS **3,996** CITATIONS
SEE PROFILE

Alexander G Stepanov
Boreskov Institute of Catalysis
136 PUBLICATIONS **1,671** CITATIONS
SEE PROFILE

THE JOURNAL OF PHYSICAL CHEMISTRY C

Article

pubs.acs.org/JPCC

Rotational and Translational Motion of Benzene in ZIF-8 Studied by ^{2}H NMR: Estimation of Microscopic Self-Diffusivity and Its Comparison with Macroscopic Measurements

Daniil I. Kolokolov,[†,‡] Lisa Diestel,[§] Juergen Caro,[§] Dieter Freude,[∥] and Alexander G. Stepanov*[,†,‡]

[†]Boreskov Institute of Catalysis, Siberian Branch of the Russian Academy of Sciences, Prospekt Akademika Lavrentieva 5, Novosibirsk 630090, Russia

[‡]Faculty of Natural Sciences, Department of Physical Chemistry, Novosibirsk State University, Pirogova Street 2, Novosibirsk 630090, Russia

[§]Institute of Physical Chemistry and Electrochemistry, Leibniz University Hannover, Callinstrasse 3A, 30167 Hannover, Germany

[∥]Universität Leipzig, Fakultät für Physik und Geowissenschaften, Linnéstrasse 5, 04103 Leipzig, Germany

Supporting Information

ABSTRACT: In relation to unique properties of metal−organic framework (MOF) ZIF-8 to adsorb and separate hydrocarbons with kinetic diameters notably larger than the entrance windows of the porous system of this microporous material, the molecular dynamics of benzene adsorbed on ZIF-8 has been characterized and quantified with ^{2}H nuclear magnetic resonance. We have established that within the ZIF-8 cage the benzene molecule undergoes fast rotations, hovering in the symmetric potential of the spherical cage and relatively slow isotropic reorientations by collisions with the walls. Benzene performs also translational jump diffusion between neighboring cages characterized by an activation barrier E_D = 38 kJ mol^{-1} and a pre-exponential factor $\tau_{D0} = 4 \times 10^{-10}$ s. This microscopic measurement of benzene mobility allows us to estimate the self-diffusion coefficient for benzene in ZIF-8 ($D^0_{self} \approx 4 \times 10^{-16}$ m^2 s^{-1} at T = 323 K). Macroscopic measurements of diffusivities derived from membrane permeation studies (3.5×10^{-15} m^2 s^{-1} at T = 298 K for fractional occupancy $\Theta \approx 0.99$) and sorption uptake ($D_{i,MS} \approx 10^{-20}$ m^2 s^{-1} at 323 K) are several orders of magnitude larger or smaller than the microscopic self-diffusion coefficient D^0_{self}, which was derived from relaxation time analysis. This experimental finding is attributed to the limits of macroscopic measurements.

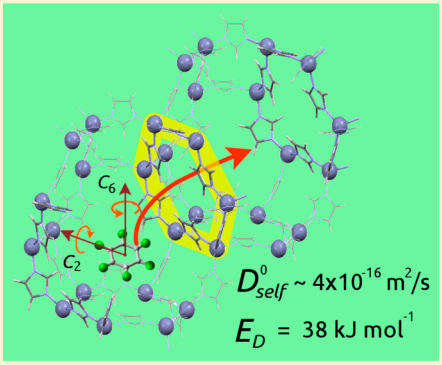

1. INTRODUCTION

Zeolitic imidazolate frameworks (ZIFs) are an important subclass of metal−organic framework (MOF) materials, characterized by zeolite-like topologies.[1,2] Such framework organization coupled with very high pore volume, exceptional for a MOF chemical and thermal stability (up to ∼550 °C) and tunable organic building blocks, make them highly attractive for applications as gas storage, chemicals encapsulation, sensing, and separation.[3−7]

Although about 100 different ZIF structures were already discovered, one of the most studied is ZIF-8.[1,2] It is composed of zinc cations coordinated to four 2-methylimidazolate ligands, resulting in a hybrid material with sodalite topology (SOD) with large spherical cavities of ∼11.6 Å diameter connected by small windows with a dimension of ∼3.4 Å.

Such framework composition makes ZIF-8 particularly interesting as a molecular sieve. Indeed it was demonstrated recently that ZIF-8 is capable to separate light paraffins/olefins with high selectivity.[8] These results stimulated further adsorption and membrane permeation studies that revealed ZIF-8 was capable to fit molecules like linear and branched alkanes[9] with kinetic diameter of $d_{crit} \approx 4.3$ Å and even larger aromatic molecules with $d_{crit} \approx 5$ Å.[6,10] This spectacular effect was related to the "flexibility" of the framework.

The MOF type materials are remarkable to show different kinds of flexibility including the (i) substantial change of the unit cell size, called "breathing",[11−13] (ii) small or no change of the unit cell size for linker reorientation, called "gate opening",[14−17] and (iii) the overcoming of the window barrier by slightly larger molecules with sufficient kinetic energy under consideration of lattice vibrations.[18,19] However, for molecules with critical diameters larger than 3.4 Å (Rietveld pore opening of ZIF-8), the gate opening is most likely the key phenomenon. Indeed, the application of excessive pressure, temperature, or adsorption of guest molecules was demonstrated to induce deformations of linker orientation relative to their equilibrium position.[14,20,21] Pirngruber et al.[9] described this gate opening effect as the "transitory tilt" of the imidazolate ligands, which allows to increase the formal pore window size of 3.4 Å by almost the factor of 2 and tried to correlate this phenomenon

Received: March 18, 2014
Revised: May 15, 2014
Published: May 29, 2014

   dx.doi.org/10.1021/jp5026834 | J. Phys. Chem. C 2014, 118, 12873−12879

with separation of *n*-alkanes/aromatic molecules by ZIF-8 in breakthrough experiments.[10] This linker "tilting" also qualitatively explains the relatively high value of the flux of benzene ($N_{benzene} \approx 3.6 \times 10^{-7}$ mol min^{-1} cm^{-2}) permeating through the ZIF-8 membrane.[22]

However, despite the importance of the problem and numerous macroscopic measurements, no *microscopic* study of the molecular dynamics of benzene inside the ZIF-8 pores was reported yet. Moreover, the only attempt to estimate the diffusion of aromatic molecules inside ZIF-8 was made by gas phase sorption uptake experiments.[6] These macroscopic measurements estimated a rather low corrected diffusivity of $D^0_{trans} \sim 10^{-20}$ m^2 s^{-1} for a loading ~1 molecule per cage at 323 K, with a relative high activation energy $E_{Dtrans} \sim 40$ kJ mol^{-1}. These corrected diffusivities from macroscopic studies should be comparable with self-diffusivities derived from microscopic studies.

Measuring such slow translational dynamics, and differentiating it from fast internal rotations expected for adsorbed benzene, is not a trivial task, and we need some adequate experimental tool. A particularly good solution could be provided by solid-state ^{2}H nuclear magnetic resonance (NMR) since it covers a very broad time scale of molecular motions, 10^{-4}−10^{-10} s. ^{2}H NMR line shape is very sensitive to the mode and the rate of the motion in which the molecule is involved.[23−26] Therefore, ^{2}H NMR patterns can be used to probe the actual mechanism of reorientational motion and thus serve as a marker of the molecule surrounding in the confined area. Benzene as the basic and most important representative among aromatic molecules is often used as a model guest to probe molecular interactions and organization in different classes of porous materials. So far the benzene dynamics was characterized by ^{2}H NMR in bulk/condensed state[27,28] and adsorbed into mesoporous silica gels,[28,29] active alumina,[30,31] graphite,[32] zeolites,[33−38] and MOFs.[39] Those results clearly demonstrated that benzene mobility was extremely sensitive to the inner potential provided by the interior of porous material.

In this work we report the successful use of ^{2}H NMR technique to probe molecular mobility of benzene inside the ZIF-8 micropores and estimate the time scale of rotational and translational motion of adsorbed benzene. For correlation, also macroscopic measurements of benzene pervaporation through ZIF-8 membranes have been performed and the derived transport diffusion coefficient can be compared with the microscopic estimation of the self-diffusivity derived from ^{2}H NMR relaxation measurements.

2. EXPERIMENTAL SECTION

2.1. Materials. Nanocrystals of ZIF-8 have been prepared following the recipe of Cravillon et al.[40] First, 0.73 g of $ZnNO_3 \cdot 6H_2O$ (2.45 mmol, 1 equiv) in 50 mL of methanol and 0.81 g of 2-methylimidazole (9.86 mmol, 1 equiv) in 50 mL of methanol were mixed under vigorous stirring and stored for 2 h at room temperature. The precipitate was collected by centrifugation and washed twice with 50 mL of methanol. Further material was dried in nitrogen at 373 K overnight. X-ray diffraction analysis (XRD) proved that it was pure ZIF-8 with a crystal size of 40 nm. SEM image of the nanosized ZIF-8 and the corresponding XRD pattern are given in the Supporting Information.

Perdeuterated benzene-d_6 with 99.6% ^{2}H isotope enrichment purchased from Sigma-Aldrich Inc. was used in this work.

2.2. Sample Preparation. In order to prepare a sample for the NMR experiments, approximately 0.064 g of ZIF-8 powder was loaded in a glass tube, 5 mm outer diameter, and connected to a vacuum system. The sample was then heated at 423 K for 8 h under vacuum to a final pressure above the sample of 10^{-2} Pa. After cooling the sample back to room temperature, the material was exposed to the vapor of previously degassed benzene-d_6 (30 mbar) in the calibrated volume (38.7 mL). It took ~20 min for complete consumption of benzene-d_6 vapor to occur (4 mg of benzene was adsorbed). The quantity of adsorbed benzene corresponded to 1 molecule per cavity of ZIF-8. After adsorption, the neck of the tube was sealed off, while the material sample was maintained in liquid nitrogen in order to prevent its heating by the flame. The sealed sample was then transferred into the NMR probe.

2.3. NMR Measurements. ^{2}H NMR experiments were performed at the Larmor frequency $\omega_z/2\pi = 61.42$ MHz on a Bruker Avance-400 spectrometer, using a high power probe with 5 mm horizontal solenoid coil. All ^{2}H NMR spectra were obtained by Fourier transformation of quadrature-detected phase-cycled quadrupole echoes arising in the pulse sequence $(90°_x - \tau_1 - 90°_y - \tau_2 - \text{acquisition} - t)$, where $\tau_1 = 20$ μs, $\tau_2 = 21$ μs, and t is a repetition time of the sequence during the accumulation of the NMR signal.[41] The duration of the $\pi/2$ pulse was 1.8−2.1 μs. Spectra were typically obtained with 500−1000 scans with repetition time ranging from 1 to 10 s. Inversion−recovery experiments for determination of the spin−lattice relaxation times (T_1) were carried out using the pulse sequence $(180°_x - \tau_v - 90°_{\pm x} - \text{acquisition} - t)$, where τ_v was a variable delay between the 180° and 90° pulses. T_2 values were derived from the Lorentzian-type spectra according to the well-known relation $T_2 = 1/\pi\Delta\nu_{1/2}$, where $\Delta\nu_{1/2}$ is the width at a half-height of the Lorentzian line shape. Some experimental values of T_2 were additionally measured by a Carr−Purcell−Meiboom−Gill (CPMG)[42] pulse sequence. A good coincidence of T_2 measured with CPMG with that derived from the line width was found. T_1 values were measured with an accuracy of 5−8%, while the estimation of the accuracy of T_2 values are in a 7−10% interval with regard to the measured values.

The temperature of the samples was controlled with a flow of nitrogen gas, stabilized with a variable-temperature unit BVT-3000 with a precision of about 1 K.

3. RESULTS AND DISCUSSION

3.1. Mobility Characterization and Estimation of Benzene Self-Diffusivity with ^{2}H NMR. Figure 1 shows ^{2}H NMR line shapes expected for benzene molecule involved in different reorientational motions. The actual reorientation mechanism of benzene molecules depends strongly on environmental media. In the gas state, the benzene molecule represents an axially symmetric rotor with the rotation around the C_6 symmetry axis being the most favorable. In the solid state, the benzene molecule is immobile on the ^{2}H NMR time scale (i.e., $\tau_c > 10^{-6}$ s) only below 90 K,[27,28] exhibiting the line shape like that shown in Figure 1a. At the temperature as high as 100 K the molecules of solid benzene become involved in the rotation around their C_6 axes with the line shape shown in Figure 1b, and this rotation is retained up to the melting point of benzene.[27,28]

The presence of other modes of benzene molecule reorientation, including the random isotropic reorientation, depends strongly on the particular system. The ^{2}H NMR line shape of benzene adsorbed in ZSM-5 cannot be described by

dx.doi.org/10.1021/jp5026834 | J. Phys. Chem. C 2014, 118, 12873−12879

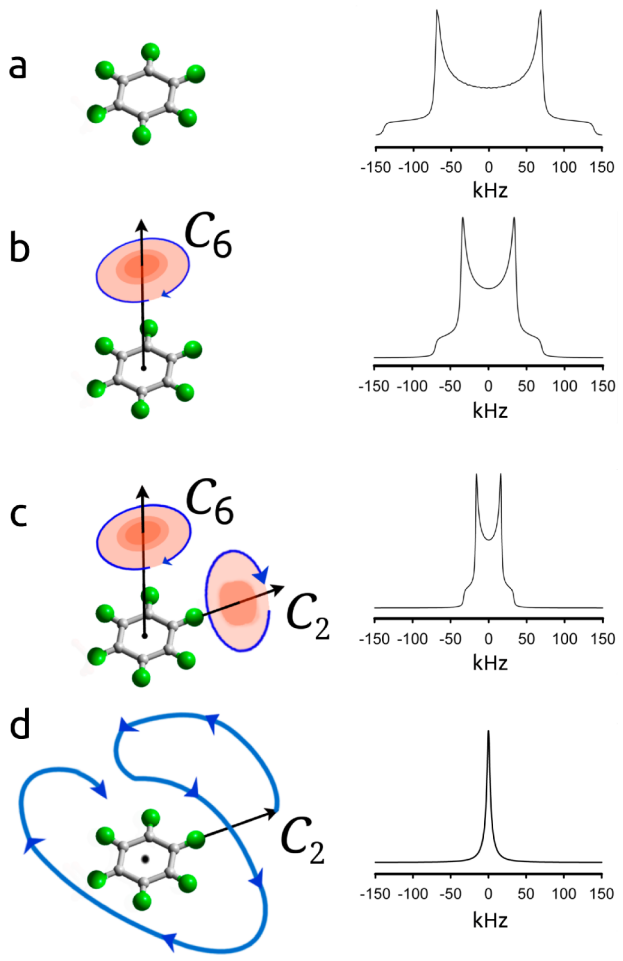

Figure 1. Theoretical ^{2}H NMR line shapes for deuterated benzene molecules undergoing different types of motion: static molecules (a); fast planar rotation around C_6 symmetry axis (b); fast rotation around both C_6 and C_2 axes (c); and fast isotropic reorientation (d).

isotropic reorientation at temperatures $T < 440$ K.[37] However, it can be described by an isotropic motion at $T > 200$ K in SBA-15,[28] Al_2O_3,[43] and NaX zeolite[33,36] since Lorentzian type line shapes were observed in these cases. Below 200 K, the random reorientation of benzene is very slow ($\tau_c > 10^{-4}$ s) in the porous materials mentioned above, even in MIL-47(V) type material with relatively large pores (~10 Å × 10 Å) and low loading of 1 molecule per MOF unit cell.[39]

Figure 2 shows the evolution of the ^{2}H NMR spectra of benzene-d_6 adsorbed on ZIF-8 in dependence of the temperature. Contrary to other adsorptive systems reported so far,[28,33,36,37,43] the adsorbed benzene exhibits a Lorentzian line shape already at $T \approx 100$ K. This indicates that benzene in ZIF-8 is involved in isotropic motion already at a temperature as low as 100 K. Such results is a direct spectroscopic evidence that benzene molecules are indeed isolated from each other and rapidly isotropically rotating, hovering in the internal potential of the cavity like a weakly bonded molecular top. From this finding by ^{2}H NMR we can conclude that the benzene molecules have entered the ZIF-8 pore system and do not form any surface layer on the outer surface of the ZIF-8 nanocrystallites.

The information on benzene dynamics in ZIF-8 can be obtained from the analysis of the spin–lattice (T_1) and spin–spin (T_2) relaxation times as a function of temperature (Figure 3). The behavior of two curves for T_1 and T_2 shows that, in contrast with a typical liquid state situation,[44] the benzene molecules in ZIF-8 framework exhibit both (i) very fast motional modes, governing the T_1 relaxation times, and (ii) much slower modes that affect the transverse relaxation T_2. Such behavior of T_1 and T_2 was already observed for linear alkanes in 5A zeolite with a cavity–window–cavity structural topology similar to ZIF-8.[45]

T_1 smoothly changes with temperature without any bending of the curve within the temperature range of 100–400 K. This means that the relaxation is regulated in this temperature window by a single fast motional mode. However, at 450 K the T_1 stops to further increase and tends to decrease with

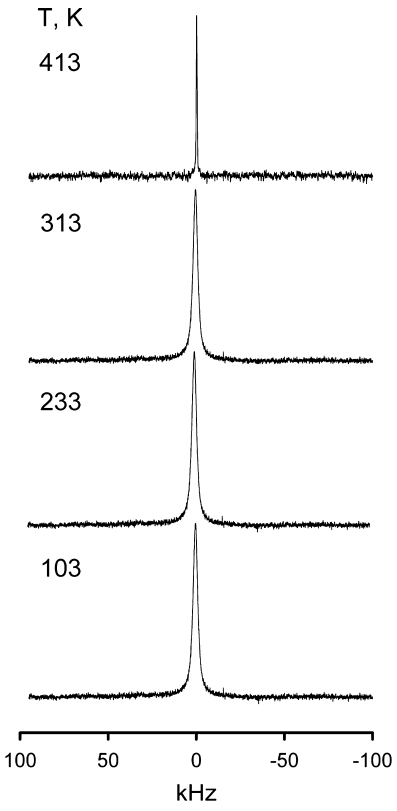

Figure 2. Evolution with temperature of ^{2}H NMR spectrum of benzene-d_6 adsorbed on ZIF-8 with loading of ~1 molecule per cavity.

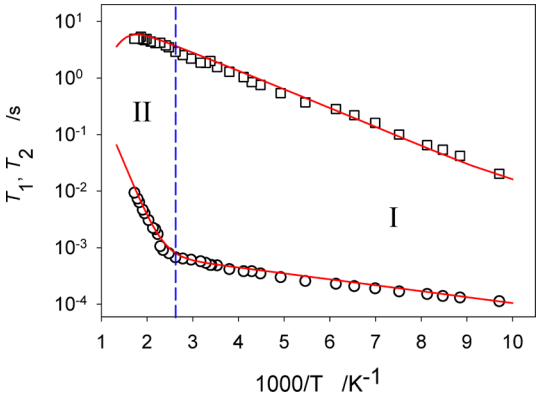

Figure 3. Temperature dependences of ^{2}H NMR T_1 (□) and T_2 (○) relaxation times for benzene-d_6 adsorbed in ZIF-8.

dx.doi.org/10.1021/jp5026834 | J. Phys. Chem. C 2014, 118, 12873–12879

temperature, which indicates the presence of another motional mode.

T_2 relaxation shows clearly two regions of its evolution with temperature. In the temperature region I from 100 to 400 K, the evolution of T_2 is characterized by a very low slope, and in the temperature region II between 400 and 500 K, with a much steeper monotonic growth. Thus, we have again two motional modes that define the T_2 evolution with temperature. It is important to note that the evolution of T_2 in the temperature region II is clearly meeting the change of evolution of T_1 in temperature region II. This indicates that both T_1 and T_2 evolutions in the temperature region II reflect essentially the same motion. In order to correctly describe the experimental results we need a dynamical model that can fit both relaxation curves simultaneously.

Let us first deal with the T_1 relaxation. The spin−lattice relaxation is most sensitive to motions with characteristic time $\sim\omega_z^{-1}$, i.e., $\sim 10^{-9}$ s, for our experimental conditions. Since T_1 evolves smoothly between 100 and 450 K we can assume that only one internal fast motion controls the molecular motion of adsorbed benzene. It can be assumed that this fast motion represents the rotation of the benzene ring around its C_6 axis. However, our fitting test for T_1 and T_2 has shown (see Supporting Information, Figure S1) that one cannot fit both experimental curves, provided that the T_1 curve reflects only a single fast rotation. So we have to assume in addition to the fast C_6 another more slow rotation around the C_2 symmetry axis. Since we could not estimate the parameters of the C_6 rotation, we have assumed that the kinetics of the rotation around C_6 axis is similar to those measured for benzene in MOF MIL-47 system[39] (E_{C_6} = 3 kJ mol^{-1}; $\tau_{C_60} \approx 10^{-13}$ s). We have to note, however, that the parameters of the C_6 rotation were not essential for T_1 and T_2 curves fitting, provided that benzene is involved in a second, much slower rotation around its C_2 axis. It follows that the parameters of C_6 rotation just have to be at least 10 times faster at 100 K than the second rotation around C_2 axis. We have inferred that the rotation around C_2 axis is responsible for the observed T_1 relaxation curve with fitting parameters E_{C_2} = 6.5 kJ mol^{-1} and $\tau_{C_20} = 1.6 \times 10^{-12}$ s. The geometry of this rotation is defined by the benzene geometry (see Supporting Information for fitting details).

The situation for the T_2 relaxation is more complicated. Adsorbed benzene exhibits a liquid-like line shape. This means that T_2 is defined by an isotropic reorientation of benzene molecules. However, the fast internal rotations of benzene alone are not able to explain the observed isotropic pattern. So some additional motion of benzene must exist. This isotropic reorientation can arise basically from two types of motion. The first one is the random collision of benzene molecules with the walls within one cage of ZIF-8, and the second one is the translational migration of benzene over the pore system, e.g., by jumps from cage to cage passing the window. The second motion could be considered as translational jump diffusion with a self-diffusion coefficient D^0_{self}. It can be assumed that reorientation by collisions with cage walls could be characterized by a small activation barrier and thus governs the temperature region I of the T_2 relaxation curve. The translational jump diffusion through narrow "gates" could require much higher activation energy. Therefore, it is fast enough only at relatively high temperatures.

The relaxation model that takes into account four different modes of benzene motion in ZIF-8 allows us to perfectly fit simultaneously both T_1 and T_2 experimental curves. Reorientation by random collision with cage walls is characterized by a very low activation barrier E_R = 2 kJ mol^{-1} and a rather high pre-exponential factor $\tau_{R0} = 10^{-5}$ s. Such long characteristic time indicates that either this motion is not very effective in terms of random reorientation or that the benzene molecule is literally suspended in the spherical potential of the ZIF-8 cavity. Its collisions with walls are quite rare, compared to internal rotations. The translational motion by jumps between the cages is characterized by an activation barrier of E_D = 38 kJ mol^{-1} and a pre-exponential factor $\tau_{D0} = 4 \times 10^{-10}$ s as derived from T_1 and T_2 fitting. Such parameters of translational motion indicate that we are indeed monitoring the microscopic, local diffusion between the cages. This is essentially the main result of the present study.

Having got the kinetic parameters for translational diffusion characteristic time τ_{D0}, we can estimate the self-diffusion coefficient D^0_{self} of benzene in ZIF-8 and compare it with results of macroscopic measurements. Assuming that the diffusion occurs by jumps between the centers of the cages, the self-diffusion coefficient D^0_{self} can be estimated from Einstein equation $D^0_{self} = \langle l \rangle^2/6\tau_D$, where l is the mean distance between the centers of neighboring cages and τ_D is the mean residence time of the molecule in the cage. We have estimated from this equation that $D^0_{self} \approx 4 \times 10^{-16}$ m^2 s^{-1} at 323 K. Such low diffusivity can hardly be monitored by pulsed-field gradient (PFG) NMR. The arguments for this are described in the following paragraph.

The PFG NMR diffusometry determines the self-diffusion coefficient D by measuring the decay of the amplitude S (S_0 for zero gradient) of a stimulated echo in dependence of the field gradient intensity g by the well-known equation (see ref 47) $\psi = S/S_0 = \exp[-D(\delta g\gamma)^2(\Delta - (\delta/3))]$. Here, δ denotes the gradient pulse duration and Δ is the observation time between the first and third $\pi/2$ pulses of the stimulated echo pulse sequence. The value of the gyromagnetic ratio amounts for ^{1}H nuclei $\gamma = 26.7522128 \times 10^7$ s^{-1} T^{-1}. We consider now benzene in ZIF-8 at 323 K with our experimentally estimated self-diffusion coefficient of $D^0_{self} \approx 4 \times 10^{-16}$ m^2 s^{-1}. In order to calculate the expected PFG NMR echo decay for the benzene, we use a gradient pulse duration of 1 ms, which has to be shorter than the transverse relaxation time (the experimentally under MAS determined value is 2.9 ms), and an observation time of 1s, which has to be shorter than the experimentally obtained longitudinal relaxation time of 2 s. In addition, we assume a maximum gradient of 50 T m^{-1}. Then we obtain $\psi \approx 0.07$. However, a value of $\psi \approx 1$ is necessary for the accurate determination of the self-diffusion coefficient by PFG NMR. A maximum gradient of about 200 T m^{-1} would be needed, but is not yet realized in PFG NMR diffusometry.

Hence, because of the impossibility to measure the self-diffusion coefficient by PFG NMR for benzene in ZIF-8, we further compared our ^{2}H NMR relaxation estimate of self-diffusivity with diffusion coefficients derived from (i) membrane permeation and (ii) sorption uptake.

3.2. Determination of Transport Diffusion Coefficient from Pervaporation Studies of Benzene through ZIF-8 Membrane. ZIF-8 membrane has been grown as a supported dense layer on top of a porous ceramic as shown in Figure 4, and pervaporation studies of benzene on this membrane have been carried out. Details of the membrane synthesis and pervaporation are given in ref 22 and in the Supporting Information.

dx.doi.org/10.1021/jp5026834 | J. Phys. Chem. C 2014, 118, 12873−12879

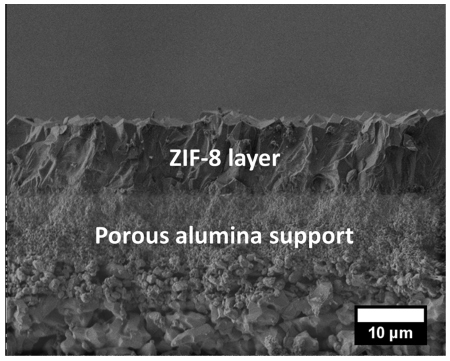

Figure 4. Cross section of a 15 μm ZIF-8 membrane on a ceramic macroporous support.

In single component benzene pervaporation experiments, a benzene flux of $N_{benzene} \approx 3.6 \times 10^{-7}$ mol min^{-1} cm^{-2} through the ZIF-8 membrane has been measured at room temperature. From these pervaporation experiments, Fickian or "transport" diffusion coefficients $D_{i,Fick}$ and Maxwell–Stefan or "corrected" diffusion coefficients $D_{i,MS}$ can be derived (for details, see the Supporting Information).

According to refs 46 and 47 for constant driving force, the first Fickian Law gives the permeation flux density N_i.

$$N_i = -D_{i,Fick} \nabla q_i \quad (1)$$

with ∇q_i as the gradient of the molar loading. $D_{i,Fick}$ is related to the $D_{i,MS}$ by the thermodynamic factor Γ_i.[48]

$$D_{i,Fick} = D_{i,MS} \Gamma_i \quad (2)$$

Γ_i characterizes the curvature of the adsorption isotherm and is defined by

$$\Gamma_i = \frac{q_i}{p_i} \frac{dp_i}{dc_i} = \frac{d \ln p_i}{d \ln q_i} \quad (3)$$

If the adsorption system behaves ideally, i.e., if there is a linear (Henry) adsorption isotherm, d ln p_i/d ln q_i becomes 1, and under this condition, the Fickian or "transport" diffusivity is equal to the Maxwell–Stefan or "corrected" diffusivity (ref 47).

Molecular dynamics simulation showed that at zero loading the three diffusion coefficients $D_{i,Fick}$, $D_{i,MS}$, and the self-diffusion coefficient D^0_{self} were identical but with increasing loading $D_{i,Fick} > D_{i,MS} \geq D^0_{self}$. However, for most adsorbate systems the self- and Maxwell–Stefan diffusion coefficients become similar again at high loadings[46] since at pore saturation the correlation effects become dominant. Krishna[49] showed for mixtures that, as the concentration of guest molecules within the pores approached saturation, the molecular jumps became increasingly correlated. When substituting in a thought experiment the binary mixture components by tagged and untagged species, this virtual experiment leads to the physically expected and mathematically exact relationship $D^0_{self} = D_{i,MS}$.[50]

For the flux density N_i, eq 1 can be simplified to

$$N_i = \frac{\varepsilon \rho q_{sat}}{\delta} D_{i,MS} \Gamma_i (\Theta_{feed} - \Theta_{permeate}) \quad (4)$$

with the membrane porosity $\varepsilon = 0.62$, the ZIF-8 framework density $\rho = 924$ kg m^{-3}, the saturation capacity for benzene $q_{sat} = 4.5$ mol kg^{-1}, the ZIF-8 membrane thickness $\delta = 15$ μm, and the thermodynamic factor Γ_i. For a single-site Langmuir isotherm, eq 3 gives $\Gamma_i = 1/(1 - \Theta_i)$ with Θ as the fractional occupancy. Published isotherm data of benzene in ZIF-8[51] can be used for the calculation of Γ_i. As a rough estimate, the downstream fractional loading of the membrane can be assumed to be zero, i.e., $\Theta_{permeate} = 0$. By assuming different values of fractional occupancy Θ_i on the upstream side of the membrane, the corresponding $D_{i,MS}$ can be calculated. As outlined above, for high loadings, the Maxwell–Stefan diffusivity $D_{i,MS}$ derived from pervaporation studies should come near to the self-diffusivity D^0_{self} estimated from NMR relaxation time experiments. This expectation is indeed found as a tendency in Figure S1, Supporting Information. However, there is still 1 order of magnitude difference between $D_{i,MS} \approx 3.5 \times 10^{-15}$ m^2 s^{-1} from pervaporation at $\Theta = 0.99$ loading and the level of $D^0_{self} \approx 4 \times 10^{-16}$ m^2 s^{-1} from NMR relaxation.

However, when comparing our result on benzene diffusivity in ZIF-8 as derived from pervaporation studies with the $D_{i,MS}$ data obtained from gas phase sorption uptake experiments,[6] we see that the activation barrier of the process is basically the same ~40 kJ mol^{-1}, whereas the corrected diffusion coefficient $D_{i,MS} \approx 10^{-20}$ m^2 s^{-1} at 323 K is several orders of magnitude smaller than the microscopic self-diffusion coefficient $D^0_{self} \approx 4 \times 10^{-16}$ m^2 s^{-1} as derived from NMR relaxation analysis, which underlines the limits of macroscopic transient uptake measurements. Often discrepancies between macroscopic and microscopic diffusivity measurements are reported, which can be explained in terms of structural defects leading to surface and intracrystalline barriers, exhibiting dramatic effects on sorption uptake kinetics on the macroscale but with only minimal influence on the microscale.[47,52]

4. CONCLUSIONS

We were able to demonstrate by means of solid-state ^{2}H NMR that the benzene molecules are indeed adsorbed inside the ZIF-8 cages proving the gate opening effect in this MOF on a microscopic level. At low loadings (~1 molecule per cage) the adsorbed benzene molecules are located in separate cages and thus isolated from each other. Within the ZIF-8 cage, the benzene molecule quickly rotates hovering in the symmetric potential of the spherical cage and performs relatively slow isotropic reorientations by collisions with its walls. Finally benzene performs translational jump diffusion between the neighboring cages with an activation barrier $E_D = 38$ kJ mol^{-1} and a pre-exponential factor $\tau_{D0} = 4 \times 10^{-10}$ s. These are the first microscopic measurements of benzene diffusivity in ZIF-type materials since the direct measurement of the slow benzene self-diffusion by pulsed field gradient NMR is not possible. Our self-diffusivity ($D^0_{self} \approx 4 \times 10^{-16}$ m^2 s^{-1} at $T = 323$ K) estimated from relaxation time analysis using the model of activated jumps between neighboring cavities lies in between the Maxwell–Stefan or "corrected" diffusivities derived from membrane permeation ($D_{i,MS} \approx 3.5 \times 10^{-15}$ m^2 s^{-1} at $T = 298$ K for fractional occupancy $\Theta \approx 0.99$) and sorption uptake studies ($D_{i,MS} \approx 10^{-20}$ m^2 s^{-1} at 323 K).

■ ASSOCIATED CONTENT

Supporting Information

Technical details on ^{2}H NMR T_1 and T_2 relaxation time simulation procedure, motion models implementation, SEM image and XRD analysis of used ZIF-8 material, ZIF-8 membrane preparation and pervaporation experiments on ZIF-8 membranes, interpretation and correlation of Fickian or "transport" diffusion coefficients, and Maxwell Stefan diffusion coefficients and self-diffusion coefficients. This

material is available free of charge via the Internet at http://pubs.acs.org.

AUTHOR INFORMATION

Corresponding Author

*(A.G.S.) Tel: +7 952 905 9559. Fax: +7 383 330 8056. E-mail: stepanov@catalysis.ru.

Notes

The authors declare no competing financial interest.

ACKNOWLEDGMENTS

This work was supported by Russian Foundation for Basic Research (Grant Nos. 14-03-91333). L.D. and J.C. thank DFG Priority Program 1362 (Porous Metal−Organic Frameworks). We are grateful to Rajamani Krishna (Van't Hoff Institute, University Amsterdam) for help in the correlation and interpretation of the different diffusion studies.

REFERENCES

(1) Huang, X. C.; Lin, Y. Y.; Zhang, J. P.; Chen, X. M. Ligand-Directed Strategy for Zeolite-Type Metal-Organic Frameworks: Zinc(II) Imidazolates with Unusual Zeolitic Topologies. *Angew. Chem., Int. Ed.* **2006**, *45*, 1557−1559.

(2) Park, K. S.; Ni, Z.; Cote, A. P.; Choi, J. Y.; Huang, R. D.; Uribe-Romo, F. J.; Chae, H. K.; O'Keeffe, M.; Yaghi, O. M. Exceptional Chemical and Thermal Stability of Zeolitic Imidazolate Frameworks. *Proc. Natl. Acad. Sci. U.S.A.* **2006**, *103*, 10186−10191.

(3) Chen, B. L.; Liang, C. D.; Yang, J.; Contreras, D. S.; Clancy, Y. L.; Lobkovsky, E. B.; Yaghi, O. M.; Dai, S. A Microporous Metal-Organic Framework for Gas-Chromatographic Separation of Alkanes. *Angew. Chem., Int. Ed.* **2006**, *45*, 1390−1393.

(4) Férey, G. Hybrid Porous Solids: Past, Present, Future. *Chem. Soc. Rev.* **2008**, *37*, 191−214.

(5) Cunha, D.; Ben Yahia, M.; Hall, S.; Miller, S. R.; Chevreau, H.; Elkaim, E.; Maurin, G.; Horcajada, P.; Serre, C. Rationale of Drug Encapsulation and Release from Biocompatible Porous Metal−Organic Frameworks. *Chem. Mater.* **2013**, *25*, 2767−2776.

(6) Zhang, K.; Lively, R. P.; Zhang, C.; Chance, R. R.; Koros, W. J.; Sholl, D. S.; Nair, S. Exploring the Framework Hydrophobicity and Flexibility of ZIF-8: From Biofuel Recovery to Hydrocarbon Separations. *J. Phys. Chem. Lett.* **2013**, *4*, 3618−3622.

(7) Bae, T. H.; Lee, J. S.; Qiu, W. L.; Koros, W. J.; Jones, C. W.; Nair, S. A High-Performance Gas-Separation Membrane Containing Submicrometer-Sized Metal-Organic Framework Crystals. *Angew. Chem., Int. Ed.* **2010**, *49*, 9863−9866.

(8) Bohme, U.; Barth, B.; Paula, C.; Kuhnt, A.; Schwieger, W.; Mundstock, A.; Caro, J.; Hartmann, M. Ethene/Ethane and Propene/Propane Separation via the Olefin and Paraffin Selective Metal−Organic Framework Adsorbents CPO-27 and ZIF-8. *Langmuir* **2013**, *29*, 8592−8600.

(9) Peralta, D.; Chaplais, G.; Simon-Masseron, A.; Barthelet, K.; Chizallet, C.; Quoineaud, A. A.; Pirngruber, G. D. Comparison of the Behavior of Metal−Organic Frameworks and Zeolites for Hydrocarbon Separations. *J. Am. Chem. Soc.* **2012**, *134*, 8115−8126.

(10) Peralta, D.; Chaplais, G.; Paillaud, J. L.; Simon-Masseron, A.; Barthelet, K.; Pirngruberb, G. D. The Separation of Xylene Isomers by ZIF-8: A Demonstration of the Extraordinary Flexibility of the ZIF-8 Framework. *Microporous Mesoporous Mater.* **2013**, *173*, 1−5.

(11) Kitagawa, S.; Uemura, K. Dynamic Porous Properties of Coordination Polymers Inspired by Hydrogen Bonds. *Chem. Soc. Rev.* **2005**, *34*, 109−119.

(12) Serre, C.; Millange, F.; Thouvenot, C.; Nogues, M.; Marsolier, G.; Louer, D.; Férey, G. Very Large Breathing Effect in the First Nanoporous Chromium(III)-Based Solids: MIL-53 or CrIII(OH), $\{O_2C\text{-}C_6H_4\text{-}CO_2\}$,$\{HO_2C\text{-}C_6H_4\text{-}CO_2H\}x,H_2Oy$. *J. Am. Chem. Soc.* **2002**, *124*, 13519−13526.

(13) Mu, B.; Li, F.; Huang, Y. G.; Walton, K. S. Breathing Effects of CO_2 Adsorption on a Flexible 3D Lanthanide Metal−Organic Framework. *J. Mater. Chem.* **2012**, *22*, 10172−10178.

(14) Fairen-Jimenez, D.; Moggach, S. A.; Wharmby, M. T.; Wright, P. A.; Parsons, S.; Duren, T. Opening the Gate: Framework Flexibility in ZIF-8 Explored by Experiments and Simulations. *J. Am. Chem. Soc.* **2011**, *133*, 8900−8902.

(15) van den Bergh, J.; Gucuyener, C.; Pidko, E. A.; Hensen, E. J. M.; Gascon, J.; Kapteijn, F. Understanding the Anomalous Alkane Selectivity of ZIF-7 in the Separation of Light Alkane/Alkene Mixtures. *Chem.—Eur. J.* **2011**, *17*, 8832−8840.

(16) Aguado, S.; Bergeret, G.; Titus, M. P.; Moizan, V.; Nieto-Draghi, C.; Bats, N.; Farrusseng, D. Guest-Induced Gate-Opening of a Zeolite Imidazolate Framework. *New J. Chem.* **2011**, *35*, 546−550.

(17) Gucuyener, C.; van den Bergh, J.; Gascon, J.; Kapteijn, F. Ethane/Ethene Separation Turned on Its Head: Selective Ethane Adsorption on the Metal−Organic Framework ZIF-7 through a Gate-Opening Mechanism. *J. Am. Chem. Soc.* **2010**, *132*, 17704−17706.

(18) Haldoupis, E.; Watanabe, T.; Nair, S.; Sholl, D. S. Quantifying Large Effects of Framework Flexibility on Diffusion in MOFs: CH_4 and CO_2 in ZIF-8. *ChemPhysChem* **2012**, *13*, 3449−3452.

(19) Chokbunpiam, T.; Chanajaree, R.; Saengsawang, O.; Reimann, S.; Chmelik, C.; Fritzsche, S.; Caro, J.; Remsungnen, T.; Hannongbua, S. The Importance of Lattice Flexibility for the Migration of Ethane in ZIF-8: Molecular Dynamics Simulations. *Microporous Mesoporous Mater.* **2013**, *174*, 126−134.

(20) Pera-Titus, M.; Lescouet, T.; Aguado, S.; Farrusseng, D. Quantitative Characterization of Breathing upon Adsorption for a Series of Amino-Functionalized MIL-53. *J. Phys. Chem. C* **2012**, *116*, 9507−9516.

(21) Finsy, V.; Kirschhock, C. E. A.; Vedts, G.; Maes, M.; Alaerts, L.; De Vos, D. E.; Baron, G. V.; Denayer, J. F. M. Framework Breathing in the Vapour-Phase Adsorption and Separation of Xylene Isomers with the Metal−Organic Framework MIL-53. *Chem.—Eur. J.* **2009**, *15*, 7724−7731.

(22) Diestel, L.; Bux, H.; Wachsmuth, D.; Caro, J. Pervaporation Studies of *n*-Hexane, Benzene, Mesitylene and Their Mixtures on Zeolitic Imidazolate Framework-8 Membranes. *Microporous Mesoporous Mater.* **2012**, *164*, 288−293.

(23) Spiess, H. W. Rotation of Molecules and Nuclear Spin Relaxation. In *NMR Basic Principles and Progress*; Diehl, P., Fluck, E., Kosfeld, R., Eds.; Springer-Verlag: New York, 1978; Vol. *15*, p 55.

(24) Smith, I. C. P. Deuterium NMR. In *NMR of Newly Accessible Nuclei*; Laszlo, P., Ed.; Academic Press: London, U.K., 1983; Vol. *2*, p 1.

(25) Jelinski, L. W. Deuterium NMR of Solid Polymers. In *High Resolution NMR Spectroscopy of Synthetic Polymers in Bulk (Methods and Stereochemical Analysis)*; Komoroski, R. A., Ed.; VCH Publishers: New York, 1986; Vol. *7*, p 335.

(26) Barnes, R. G. Deutron Quadrupole Coupling Tensors in Solids. *Adv. Nucl. Quadrupole Reson.* **1974**, *1*, 335−355.

(27) Ok, J. H.; Vold, R. R.; Vold, R. L.; Etter, M. C. Deuterium Nuclear Magnetic-Resonance Measurements of Rotation and Libration of Benzene in a Solid-State Cyclamer. *J. Phys. Chem.* **1989**, *93*, 7618−7624.

(28) Gedat, E.; Schreiber, A.; Albrecht, J.; Emmler, T.; Shenderovich, I.; Findenegg, G. H.; Limbach, H. H.; Buntkowsky, G. ^2H Solid-State NMR Study of Benzene-d_6 Confined in Mesoporous Silica SBA-15. *J. Phys. Chem. B* **2002**, *106*, 1977−1984.

(29) Zibrowius, B.; Bulow, M.; Pfeifer, H. Microdynamical Behavior of Benzene Molecules Adsorbed on Silicalite as Studied by C-13 NMR. *Chem. Phys. Lett.* **1985**, *120*, 420−423.

(30) Gottlieb, H. E.; Luz, Z. Deuterium NMR of Molecules Adsorbed on Active Alumina. *J. Magn. Reson.* **1983**, *54*, 257−271.

(31) Boddenberg, B.; Beerwerth, B. Proton and Deuteron Magnetic Resonance Relaxation of Benzene Adsorbed on Alumina and on a Platinum/Alumina Catalyst. *J. Phys. Chem.* **1989**, *93*, 1440−1447.

(32) Boddenberg, B.; Grosse, R. Deuterium NMR Study on the Rotational Dynamics and the Orientation of Benzene Molecules

Adsorbed on Graphite and Boron Nitride. *Z. Naturforsch., A: Phys. Sci.* **1986**, *41*, 1361−1368.
(33) Hasha, D. I.; Miner, V. W.; Garces, J. M.; Rocke, S. C. Dynamics of Benzene in X-Type Zeolites. *ACS Symp. Ser.* **1985**, *288*, 485−497.
(34) Eckman, R. R.; Vega, A. J. Deuterium Solid-State NMR Study of the Dynamics of Molecules Sorbed by Zeolites. *J. Phys. Chem.* **1986**, *90*, 4679−4683.
(35) Boddenberg, B.; Burmeister, R. ^{2}H NMR Study on the Rotation and Diffusion Kinetics of Propene and Benzene in NaX and Ag NaX Zeolites. *Zeolites* **1988**, *8*, 488−494.
(36) Zibrowius, B.; Caro, J.; Pfeifer, H. Deuterium Nuclear Magnetic-Resonance Studies of the Molecular-Dynamics of Benzene in Zeolites. *J. Chem. Soc., Faraday Trans. I* **1988**, *84*, 2347−2356.
(37) Kustanovich, I.; Vieth, H. M.; Luz, Z.; Vega, S. NMR-Studies of the Sorption of *p*-Xylene, Toluene, and Benzene on ZSM5 Zeolite. *J. Phys. Chem.* **1989**, *93*, 7427−7431.
(38) Geil, B.; Isfort, O.; Boddenberg, B.; Favre, D. E.; Chmelka, B. F.; Fujara, F. Reorientational and Translational Dynamics of Benzene in Zeolite NaY as Studied by One- and Two-Dimensional Exchange Spectroscopy and Static-Field-Gradient Nuclear Magnetic Resonance. *J. Chem. Phys.* **2002**, *116*, 2184−2193.
(39) Kolokolov, D. I.; Jobic, H.; Stepanov, A. G.; Ollivier, J.; Rives, S.; Maurin, G.; Devic, T.; Serre, C.; Ferey, G. Experimental and Simulation Evidence of a Corkscrew Motion for Benzene in the Metal-Organic Framework MIL-47. *J. Phys. Chem. C* **2012**, *116*, 15093−15098.
(40) Cravillon, J.; Munzer, S.; Lohmeier, S. J.; Feldhoff, A.; Huber, K.; Wiebcke, M. Rapid Room-Temperature Synthesis and Characterization of Nanocrystals of a Prototypical Zeolitic Imidazolate Framework. *Chem. Mater.* **2009**, *21*, 1410−1412.
(41) Powles, J. G.; Strange, J. H. Zero Time Resolution Nuclear Magnetic Resonance Transients in Solids. *Proc. Phys. Soc. London* **1963**, *82*, 6−15.
(42) Farrar, T. C.; Becker, E. D. *Pulse and Fourier Transform NMR. Introduction to Theory and Methods*; Academic Press: New York, 1971.
(43) Boddenberg, B.; Beerwerth, B. Proton and Deuteron Magnetic-Resonance Relaxation of Benzene Adsorbed on Alumina and on a Platimun Alumina Catalyst. *J. Phys. Chem.* **1989**, *93*, 1440−1447.
(44) Harris, R. K. *Nuclear Magnetic Resonance Spectroscopy. A Physico-Chemical View*; Pitman: London, U.K., 1983.
(45) Kolokolov, D. I.; Arzumanov, S. S.; Stepanov, A. G.; Jobic, H. Dynamics of linear n-C_6−n-C_{22} alkanes inside 5A zeolite studied by ^{2}H NMR. *J. Phys. Chem. C* **2007**, *111*, 4393−4403.
(46) Krishna, R.; van Baten, J. M. Influence of Adsorption Thermodynamics on Guest Diffusivities in Nanoporous Crystalline Materials. *Phys. Chem. Chem. Phys.* **2013**, *15*, 7994−8016.
(47) Kärger, J.; Ruthven, D. M.; Theodorou, D. N. *Diffusion in Nanoporous Materials*; Wiley-VCH: Weinheim, Germany, 2012.
(48) Krishna, R.; Wesselingh, J. A. Review Article Number 50: The Maxwell−Stefan Approach to Mass Transfer. *Chem. Eng. Sci.* **1997**, *52*, 861−911.
(49) Krishna, R.; van Baten, J. M. Describing Mixture Diffusion in Microporous Materials under Conditions of Pore Saturation. *J. Phys. Chem. C* **2010**, *114*, 11557−11563.
(50) Krishna, R. Personal information.
(51) Zhu, A. X.; Lin, R. B.; Qi, X. L.; Liu, Y.; Lin, Y. Y.; Zhang, J. P.; Chen, X. M. Zeolitic Metal Azolate Frameworks (MAFs) from ZnO/Zn(OH)(2) and Monoalkyl-Substituted Imidazoles and 1,2,4-Triazoles: Efficient Syntheses and Properties. *Microporous Mesoporous Mater.* **2012**, *157*, 42−49.
(52) Heitjans, P.; Kärger, J. *Diffusion in Condensed Matter: Methods, Materials, Models*; Springer: Berlin, Germany, 2005.